future internet

MDPI

Article

Cooperative D-GNSS Aided with Multi Attribute Decision Making Module: A Rigorous Comparative Analysis

Thanassis Mpimis [1], Theodore T. Kapsis [2], Athanasios D. Panagopoulos [2,*] and Vassilis Gikas [1]

[1] School of Rural and Surveying Engineering, National Technical University of Athens, 15780 Athens, Greece; ampimis@central.ntua.gr (T.M.); vgikas@central.ntua.gr (V.G.)
[2] School of Electrical and Computer Engineering, National Technical University of Athens, 15780 Athens, Greece; teokapsis@mail.ntua.gr
* Correspondence: thpanag@ece.ntua.gr

Abstract: Satellite positioning lies within the very core of numerous Intelligent Transportation Systems (ITS) and Future Internet applications. With the emergence of connected vehicles, the performance requirements of Global Navigation Satellite Systems (GNSS) are constantly pushed to their limits. To this end, Cooperative Positioning (CP) solutions have attracted attention in order to enhance the accuracy and reliability of low-cost GNSS receivers, especially in complex propagation environments. In this paper, the problem of efficient and robust CP employing low-cost GNSS receivers is investigated over critical ITS scenarios. By adopting a Cooperative-Differential GNSS (C-DGNSS) framework, the target's vehicle receiver can obtain Position–Velocity–Time (PVT) corrections from a neighboring vehicle and update its own position in real-time. A ranking module based on multi-attribute decision-making (MADM) algorithms is proposed for the neighboring vehicle rating and optimal selection. The considered MADM techniques are simulated with various weightings, normalization techniques, and criteria associated with positioning accuracy and reliability. The obtained criteria values are experimental GNSS measurements from several low-cost receivers. A comparative and sensitivity analysis are provided by evaluating the MADM algorithms in terms of ranking performance and robustness. The positioning data time series and the numerical results are then presented, and comments are made. Scoring-based and distance-based MADM methods perform better, while L1 RMS, HDOP, and Hz std are the most critical criteria. The multi-purpose applicability of the proposed scheme, not only for land vehicles, is also discussed.

Keywords: Intelligent Transportation Systems; Cooperative Positioning; low-cost GNSS; connected vehicles; multi-criteria decision making; ranking methods; sensitivity analysis

Citation: Mpimis, T.; Kapsis, T.T.; Panagopoulos, A.D.; Gikas, V. Cooperative D-GNSS Aided with Multi Attribute Decision Making Module: A Rigorous Comparative Analysis. *Future Internet* **2022**, *14*, 195. https://doi.org/10.3390/fi14070195

Academic Editor: Filipe Portela

Received: 27 May 2022
Accepted: 24 June 2022
Published: 27 June 2022

1. Introduction

The cornerstone of any positioning system design activity is the understanding of the user and the specific application requirements. As Global Navigation Satellite Systems (GNSS) are constantly improving, providing advanced signals and services, and GNSS receivers utilized in road sectors adopt multi-frequency, multi-constellation schemes, GNSS positioning will remain the dominant positioning service [1]. A variety of transport applications based on GNSS have been studied in practical scenarios, e.g., railways, air, and maritime transport, and geodetic networks [2–6]. Under the Intelligent Transportation Systems (ITS) umbrella lies a broad range of vehicular applications with different sets of requirements that can be categorized foremost as non-safety critical and safety-critical [7–9]. Following up, these are classified as non-connected and connected ITS (C-ITS) applications [7–9]. The adaptation of C-ITS applications implies future internet connectivity, a future road environment with minimum safety risks, maximum recourses benefits, and greener eco-driving due to lower emissions and fuel consumption [9].

Interruptions of satellite positioning regarding signal receptions in obstructed skies and complex propagation environments will require coupling with communication technologies and other sensors for more demanding applications [10,11]. Fusion with other onboard sensors, such as inertial sensors, lidars, ultra-wideband, and cameras, will be inevitable for both categories in order to fulfill the requirements of the applications [10,11]. However, Inertial Navigation System (INS)/GNSS integration can come at a prohibitive cost for mass deployment, has limited sensory coverage, and is unsuitable for small handheld devices. Similarly, Real-time Kinematic Positioning (RTK) constitutes a Differential GNSS (D-GNSS) technique to improve the positioning accuracy of the receiver but does not provide a stable solution in deep urban centers [12]. Communication technologies empower vehicle-to-everything (V2X) information share, and as they are established in the vehicle industry, a wide range of ITS applications emerge [13]. Hence, V2X and C-ITS are paving the way for Cooperative Positioning (CP) among mobile terminals but demand the highest performance levels for several metrics such as availability, accuracy, robustness, and integrity [13].

In this work, the challenge of efficient, accurate, and reliable CP that incorporates low-cost GNSS receivers in various critical ITS scenarios was addressed. The Cooperative Differential GNSS (C-DGNSS) framework was employed, which is the classical D-GNSS coupled with CP between a target vehicle and a number of surrounding candidate neighbors. All of the cars are considered connected. That means that data can be exchanged through all the vehicles and belong to a wireless network. By retaining the properties of D-GNSS, the cooperating vehicles disseminate their Position-Velocity-Time (PVT) data through radio links and GNSS corrections from the available satellites in view. The main hypothesis is that the target vehicle's low-cost receiver could improve both its relative and absolute positioning accuracy. The GNSS PVT information is comprised of National Marine Electronics Association (NMEA) messages, and the target vehicle parses the incoming NMEA sentences in a serial manner [14]. With the aid of a multi-attribute decision-making (MADM) module, the target vehicle optimally decides in real-time which neighbors to select for retrieving the GNSS corrections for improving/updating its own PVT state.

The contributions of this work are summarized as follows:

- A CP solution stemming from the C-DGNSS concept is proposed to enhance the performance of low-cost GNSS receivers in safety-critical ITS scenarios. The target's vehicle receiver can obtain GNSS corrections from a neighboring vehicle and update its own position in real-time;
- The proposed C-DGNSS methodology is aided by a MADM module that, given a variety of position-related criteria and alternative neighboring vehicles, ranks them and optimally decides which neighbor to select to retrieve PVT corrections.
- Real experimental measurements from several low-cost GNSS receivers and trajectories (experimental sessions) are provided to simulate various operating environments (i.e., deep urban, suburban, and rural areas);
- The experimental data are easily processed NMEA sentences which are manufactured universally regardless of GNSS receiver producer. The globally available NMEA data formats are fed as input (i.e., criteria values) to the considered MADM algorithms;
- Thirteen MADM algorithms are simulated with various weightings, normalization techniques, and criteria associated with positioning accuracy and reliability, such as horizontal accuracy, dilution of precision (DOP), integer ambiguity status, etc.;
- A comparative analysis is provided through an evaluation of the MADM algorithms in terms of ranking performance and robustness. An investigation of the importance and criticality of the criteria is also presented (sensitivity analysis) together with the necessary simulations' ranking results and MADM algorithms' performance tables;
- The proposed C-DGNSS algorithm will be beneficial for critical applications such as anti-collision, lane-keeping, and intersection crossing, which require high relative positioning accuracy. Moreover, it aims to improve the positioning accuracy of low-cost receivers in complex propagation environments by minimizing the operational

overheads but does not guarantee the effective minimization and elimination of user-related errors;
- The multi-purpose, generic applicability of the proposed scheme is not only for land vehicles but extends to drone positioning, swarm-of-entities guidance, drone-to-car communication, etc.

The remainder of the paper is structured as follows: in Section 2, a brief review of the ITS definitions and usages is reported, and a summary of the C-DGNSS framework on the enhancement of low-cost GNSS receivers is presented, along with the specifications for ITS positioning quality. In Section 3, the MADM theory is developed, and the employed MADM algorithms, normalization techniques, and weightings are elaborated. In Section 4, the simulation environment (trajectory, alternative vehicles, and input parameters) is described, and the MADM simulations using the experimental data take place. The ranking and numerical results are exhibited, and comments are made. Finally, Section 5 concludes the paper.

2. ITS Applications and Communication Technologies, Critical Design Requirements, and Related Works

2.1. Review of Intelligent Transportation Systems (ITS)

Next-generation mobility and transportation services demand the development of a smart, highly automated, and responsive transportation system. Such systems are known as Intelligent Transportation Systems (ITS) [7–9] and are based on Future Internet Connectivity. Their role is to facilitate the safe but efficient transportation of commodities and/or humans. This is accomplished through embedding location-based and communication information leveraged with the adoption of suitable transportation models [9]. Specifically, urban ITS aim to relieve the heavily congested and crowded city environments related to the rapid growth of automobile users in recent decades. The rapid increase in city transportation volumes drastically affects user behavior and driving style leading to an increased risk of traffic accidents [7–9].

A vehicular network constitutes a C-ITS-based network that supports interactions between the highly mobile and dynamic nodes-vehicles. In a Vehicle Ad Hoc Network (VANET), vehicles connect with each other through wireless short-range radio and with road infrastructures through either short-range radio or 3G, LTE-4G, and 5G [8,13,15]. In VANETs, by definition, vehicles act as the network nodes that are capable of transmitting (source) or receiving (destination) data, or they can even function as network routers. However, VANETs exhibit some unique features that distinguish them from other types of networks: Self-organization, high mobility (but with geographical or trajectory limitations), high transmission speed due to variable node densities, and a dynamic topology [8,13].

The vehicular networking applications are divided into (1) active road safety applications, (2) traffic efficiency and management applications, and (3) infotainment (information and entertainment) applications [15,16]. The first category is intended to decrease the probability of traffic accidents through the provision of various ITS services such as lane departure, forward collision warnings, and emergency vehicle warnings. The second category aims to improve vehicle traffic flow and coordination conditions (e.g., speed management operations) and the provision of local information and maps (e.g., cooperative navigation) [15,16]. Finally, the last category includes local cooperative services (e.g., media download and voice assistance) and global internet services [15,16].

Today, the evolution of communication technologies drives the ITS industry to connect vehicles and infrastructure, leading to Cooperative ITS (C-ITS) [8,9]. These systems offer advanced synchronized driving modalities (e.g., cooperative cruising, cooperative awareness, cooperative positioning/navigation, speed management, and cooperative sensing capabilities) [8,9]. In this case, system standardization dictates the use of interoperable protocols to enable communication among stations with various architectures. Additionally, the deployment of C-ITS demands cooperation among competing stakeholders [13,16].

The available ITS technologies come with various definitions and classifications depending on the type of nodes contributing to the communication network. Moreover, they can be classified into *vehicle-to-vehicle* (V2V), *vehicle-to-infrastructure* (V2I), *vehicle-to-nomadic* (V2N), *vehicle-to-pedestrian* (V2P), *vehicle-to-everything* (V2X), *in-vehicle network* (IVN), *vehicular ad hoc networks* (VANET), and other schemes [7,8]. In Figure 1, various ITS scenarios and connected-vehicle services are illustrated.

Figure 1. ITS scenarios and connected vehicle services.

Table 1 summarizes the various ITS wireless communication standards in terms of class and type of wireless protocol [9,17].

Table 1. Taxonomy of ITS communication technologies.

Communication Technology	Class	Wireless Standard
Dedicated short-range communications (DSRC)	Legacy	IEEE 802.11p
Vehicle Information and Communication System (VICS)	Legacy	Infrared/Microwaves
Electronic Fee Collection (EFC)	Legacy	Infrared/Microwaves
Transport and Traffic Telematics (TTT)	Legacy	Infrared/Microwaves
ITS G5	Advanced	IEEE 802.11p
Wireless Access in Vehicular Environments (WAVE)	Advanced	IEEE 802.11p
Communication Access for Land Mobiles (CALM)	Advanced	ISO 21218:2018
LTE—V2X	Advanced	LTE/4G
NR—V2X	Advanced	NR/5G

Advanced safety-critical ITS systems should fulfill a variety of operational and radio-communication requirements. From a systemic point of view, all vehicles must be uniquely identifiable, warning messages must be deliverable, and vehicle location and kinematics information (known as PVT) should be available [16]. Authentication procedures should also be evident to support links for individual and group communication [16].

In [17], an exclusive review of V2V, V2I, and V2X communications is introduced, and the role of DSRC and WAVE technologies in road safety services is mentioned. The advanced WAVE protocol based on 802.11p is designed to optimize the coordination and cooperation among vehicles and infrastructures. Similarly, the bidirectional V2I links between RFID sensors, traffic lights, cameras, lane markers, signages, and parking meters utilize DSRC frequencies to transact data. Concretely, the authors present the benefits and the challenges of the commercial employment of connected vehicle implementations, such as the financial costs and the lack of universal standardization [17].

The technical radio requirements for the three major ITS applications are included in Table 2 [12,15]. Specifically, safety-critical vehicular CP is the most demanding in

terms of the sampling rate, latency, and reliability, but the transmission rate is of less importance [12,15]. The latency requirement incorporates the propagation delay as well as the processing delay. The reliability, which is defined as the percentage of time when packets are delivered in the correct order and without losses, is very critical because the rapidly changing network topology could result in outdated/invalid position solutions.

Table 2. Taxonomy of ITS applications' technical radio requirements.

ITS Application	Sampling Rate (Hz)	Latency (ms)	Data Rate (Mbps)	Reliability (%)
Safety-critical vehicular CP	10–20	1–50	10–50	≥99.999
Traffic efficiency	1–5	50–100	50–65	≥99.9
Infotainment	On Demand	≥100	10–1000	90–99.9

2.2. Low-Cost GNSS Receivers

The Location-based Services (LBS) market is constantly growing, predicted to reach hundreds of billions of USD by 2025, while tens of billion LBS-based devices will be operating by 2025. Although high-end GNSS receivers are currently sitting on top of the positioning and navigation industry due to their high precision, accuracy, and reliability, a significant demand for low-cost and ultra-low-cost GNSS receivers will soon emerge to satisfy ITS deployment [18,19]. For instance, ITS applications, such as vehicle platooning, data transactions, and the remote control of Unmanned Aerial Vehicles (UAVs), employ low-cost LBS devices, e.g., smartphones, trackers, and wearables [9,12]. The expansion of GPS, the addition of new satellite navigation systems, and the attainment of higher sampling rates (>10 Hz) have greatly benefited low-cost GNSS receivers. They typically support a single- or dual-band functionality, have small size and mass, can operate with low-drain batteries, can form wireless networks, and are not dependent on temperature conditions while a patch-antenna is attached to them [10,18,19].

On the other hand, the commercial single-band low-cost GNSS stations are lacking in accuracy, reliability, and robustness compared to dual-band ones with geodetic antennas [18,19]. The design discrepancies between them lead to a greater radio noise/interference level, more severe multipath effects, and a decreased integer ambiguity fixing of the low-cost GNSS station. Moreover, their low availability in city environments has restricted their use, especially for vehicular, safety-critical applications. As a result, low-cost GNSS receivers alone cannot reach the full potential of satellite positioning, and, therefore, they are used complementary to other sensor types to increase redundancy and reliability in position fixing [20,21]. Many researchers have studied and proposed solutions to enhance the performance of low-cost GNSS receivers.

In [18], the authors propose a positioning apparatus comprised of two low-cost GNSS receivers placed in close proximity (up to a few cms) to model the noise and multipath errors between them. Assuming that the two GNSS stations experience identical error sources, the dual low-cost GNSS system solely evaluates the noise characteristics and mitigates the noise effects in the GNSS coordinate time series.

In [19], a real-time, continuous, low-cost positioning solution for autonomous vehicles is proposed. A single-frequency, low-cost Precise Point Positioning (PPP) GNSS receiver is integrated with an equally low-cost INS. The considered PPP/INS scheme reaches submeter root mean square (rms) accuracy in benign clear-sky environments and circumvents the navigation issues during GNSS blockages.

In [20], the authors performed kinematic experiments in rural, interurban, urban, and freeway environments to evaluate the positioning performance of a low-cost receiver using network RTK (NRTK) positioning. They achieved a centimeter-level accuracy with correction data provided from SmartNet.

Collaborative or Cooperative Positioning (CP) solutions to empower the performance of low-cost GNSS receivers in C-ITS scenarios have also been proposed. In [21], a lane–level localization tool is proposed based on infrastructure lacking CP. The participating vehicles

form vehicular sensor networks (VSNs) by equipping image sensors and are able to share lane position information through DSRC. The feasibility and successful implementation of the proposed solution met the accuracy specifications of critical ITS services.

2.3. Critical Design Requirements for C-DGNSS Applications

Safety-critical C-DGNSS applications have specific technical requirements regarding latency, reliability, and sampling rate, as exhibited in Table 2, but the networking design parameters such as the minimal and maximal Inter-Vehicle Ranges (IVRs) between the assisted vehicles, the minimum number of participating vehicles, and the interval of GNSS corrections are yet to be standardized. They strongly depend on wireless network connectivity, the mobility of the vehicles, and the local environment. In order to estimate the aforementioned requirements, further deployment, implementation, and several experimental sessions of the proposed MADM algorithm are needed, which are out of this work's scope. In deep urban areas, the streets are narrower, and so the vehicles' distances are much smaller as opposed to suburban and rural areas. Likewise, there is a greater number of candidate neighbors in deep urban environments that require more frequent corrections due to many obstructions. Therefore, the specification of the C-DGNSS is challenging and varies a lot with the local surroundings. Assuming perfect vehicle connectivity, the maximal IVRs must guarantee different multipath conditions and common satellites in view, while at least two vehicles are needed for the MADM module to be useful. Finally, the low-cost onboard receivers and the radio-link equipment must be compatible with the requirements in Table 2.

3. MADM Methodologies

In the C-DGNSS framework, the target vehicle's low-cost GNSS receiver strives to acquire GNSS corrections from the neighbor vehicles in the vicinity. Each neighbor vehicle transmits both PVT data (NMEA sentences) and corrections (Radio Technical Commission for Maritime (RTCM) Services messages). For latency-sensitive applications and critical ITS in general, it is best to rank the moving vehicles in the neighborhood and select the optimal one with which to cooperate. The ranking of moving neighbor vehicles will be estimated using only PVT data that is transmitted, while the PVT solution status of each vehicle will vary; it may be RTK-fixed or a standalone solution. After selecting the best neighbor vehicle, the target car selects to receive the corrections only from this particular neighbor vehicle and tries to estimate the integer phase ambiguities in order to improve the standard deviation of its solution. A MADM module is proposed to aid the neighbor selection using a variety of criteria, weights, and alternatives and finally rank higher a neighbor vehicle with RTK fixed solution than another standalone. MADM algorithms are computational decision-making methods that decide upon the optimal alternative or rank a specified set of alternatives [22,23].

The performance of each alternative to a specific criterion/attribute is called criterion value, and it is stored in the decision matrix of size ($P \times Q$), where P is the number of alternatives and Q is the number of criteria [22]. The derivation of the criteria weights vector is a complicated task; hence a variety of objective (e.g., entropy method) and subjective (e.g., direct rating) weighting techniques are available [22]. Additionally, the MADM algorithms are founded on linear aggregation and causality, which implies that strong inter-dependencies between criteria may disrupt the ranking outcomes. Finally, the normalization of the criteria values is a pre-processing conversion to derive a common scale and comparable input data. It is necessary to apply the right normalization techniques to facilitate the decision-making process. Given certain weighted criteria, normalized

criteria values are fed as input to the MADM module, and the sorting of the alternatives is outputted. The arrangement of the decision matrix (*D.M.*) is illustrated in (1):

$$D.M. = \begin{array}{c} \begin{matrix} C_1 & C_2 & C_3 & \dots & C_Q \end{matrix} \\ \begin{pmatrix} a_{1,1} & a_{1,2} & a_{1,3} & \dots & a_{1,Q} \\ a_{2,1} & a_{2,2} & \vdots & \vdots & a_{2,Q} \\ a_{3,1} & \vdots & \ddots & \vdots & a_{3,Q} \\ \vdots & \vdots & \vdots & \ddots & \vdots \\ a_{P,1} & a_{P,2} & a_{P,3} & \dots & a_{P,Q} \end{pmatrix} \end{array} \begin{matrix} A_1 \\ A_2 \\ A_3 \\ \vdots \\ A_P \end{matrix}, \quad (1)$$

where $A_1, A_2, A_3, \dots, A_P$ are the alternatives to be employed for decision making, $C_1, C_2, C_3, \dots, C_Q$ are the decision criteria, and $\alpha_{i,j}$ is the performance value of the i_{th} alternative with respect to the j_{th} criterion.

Currently, a wide variety of MADM methodologies and normalization techniques are available [22,23]. They can be divided according to the decision process and their common characteristics. The MADM algorithms typically employ score functions, outranking relations, hierarchy structures, and others for optimal selection. Table 3 exhibits some well-accepted and employed MADM methodologies [22,23].

Table 3. Taxonomy of main normalization techniques (P is the number of alternatives).

Normalization Technique	Benefit	Expense
Linear: Sum	$n_{ij} = \frac{a_{i,j}}{\sum_{i=1}^{P} a_{i,j}}$	$n_{ij} = \frac{1/a_{i,j}}{\sum_{i=1}^{P} 1/a_{i,j}}$
Linear: Max	$n_{ij} = \frac{a_{i,j}}{a_{j\max}}$	$n_{ij} = \frac{a_{j\min}}{a_{i,j}}$
Linear: Max−Min	$n_{ij} = \frac{a_{i,j} - a_{j\min}}{a_{j\max} - a_{j\min}}$	$n_{ij} = \frac{a_{j\max} - a_{i,j}}{a_{j\max} - a_{j\min}}$
Vector	$n_{ij} = \frac{a_{i,j}}{\sqrt{\sum_{i=1}^{P} a_{i,j}^2}}$	$n_{ij} = \frac{1/a_{i,j}}{\sqrt{\sum_{i=1}^{P} \left(1/a_{i,j}\right)^2}}$
Data Envelopment Analysis (DEA)	$n_{ij} = 1 - \frac{a_{j\max} - a_{i,j}}{\sum_{i=1}^{P} \left(a_{j\max} - a_{i,j}\right)}$	$n_{ij} = 1 - \frac{a_{i,j} - a_{j\min}}{a_{j\max}}$

The Simple Additive Weighting (SAW), Complex Proportional Assessment (COPRAS), Multi-Objective Optimization on the Basis of Ratio Analysis (MOORA), and Grey Relational Analysis (GRA) belong to the scoring-based MADM family. The scoring class is regarded to have the minimum complexity, cost, and latency and is quite readable and interpretable by the decision-makers. Moreover, the intake criteria values from the formulated decision matrix are generated, and then a scoring function is employed to output a single value for each alternative. They are most suited for the evaluation of a specific alternative than for a complete ranking. Their disadvantages are many, i.e., the idealistic assumption of linear attribute aggregation, the decision matrix normalization, the acceptance of only positive criteria values, and ranking instability in cases where the input attribute values vary greatly [22,23].

The Technique for Order of Preference by Similarity to Ideal Solution (TOPSIS), Visekriterijumsko Kompromisno Rangiranje (VIKOR), Combinative Distance-based Assessment (CODAS), Multi-Attributive Border Approximation Area Comparison (MABAC), Displaced Ideal Method (D'IDEAL), and Organization, Rangement Et. Syn-these De Donnes Relationnelles (ORESTE) belong to the distance-based MADM family. The distance-based class is regarded to have a moderate complexity, cost, and latency but high stability even at large fluctuations of the input data. This group of MADM methods calculates a pair of ideal geometric points and considers that the optimal alternative is the one that has the smallest distance from the best point and the greatest distance from the worst point; their

disadvantages are few, i.e., the decision matrix normalization and Euclidean distance are inefficient for high correlations between the criteria [22,23].

The Analytic Hierarchy Process (AHP) and Analytic Network Process (ANP) belong to the pairwise comparisons MADM family and are regarded as having significant latency, exponential complexity, computational cost, and flexibility. They demand the formulation of a three-level hierarchic structure, and the solution requires good knowledge of eigenvalues and eigenvectors. These methods mix both qualitative and quantitative data types without normalizations. However, they assume largely independent criteria, they are very biased from the subjective opinions of the decision-makers, and modifications are necessary to overcome inconsistency problems [22,23].

The Preference Ranking Organization Method for Enrichment Evaluations (PROMETHEE) and Elimination and Choice Expressing Reality (ELECTRE) belong to the outranking MADM family and are regarded as having high flexibility, rationality, and no need for any data transformations or normalizations, but they express a quadratic time complexity and are unfit for more than five criteria. They employ a preference function, e.g., Gaussian, and a number of veto thresholds to perform pairwise comparisons between a set of alternatives and derive preference flows. They can produce partial and complete rankings or select the best action based on outranking relationships [22,23].

Finally, the Multi Attribution Utility Theory (MAUT) and Multi Attribution Value Theory (MAVT) belong to the utility/valuate MADM family. They are also biased by decision-maker judgment, but they can deal with uncertainties in the data. On the other hand, they demand an immense amount of input data, and the derived results exhibit strong subjectivity [22,23].

In general, the sensitivity analysis investigates the impact of weighting, the number of alternatives, and the measurement scale on the ranking stability and hence the method's robustness [24,25]. The importance of a criterion reflects its weight's magnitude on that criterion, while the criticality is the degree of ranking variation for a small shift in the criterion's weight. Those methods that statistically retain the priorities and ranking of alternatives when altering the input data deem them to be the more robust, and consequently, they suit real-time applications. Another problem is the rank-reversal phenomenon that occurs in all classes and methods. It occurs when a duplicate alternative or a worse-scoring alternative is added, removed, or replaced, then the top ranks might reverse, which is inconsistent [22,23].

In [26], the challenge of energy-efficient network selection in wired, wireless, and public transport networks is formulated as a decision-making problem. The authors propose a MADM strategy based on users' requirements and different services (e.g., QoS, bandwidth, delay, data volume, and cost, etc.). Specifically, the AHP is applied for a heterogeneous vehicular-assisted network in the context of smart cities. Unarguably, the method's consistency constitutes a key parameter in vehicular network selections so as to achieve efficient handovers.

Due to their complex architecture, a vast quantity of input data, and strong subjectivity, the pairwise comparison techniques and utility algorithms are rejected for cooperative positioning systems operating in dynamic environments with demanding latency, reliability, and continuity requirements [23].

4. Simulation Results

4.1. Simulation Criteria and Environment Description

By means of the C-DGNSS positioning framework, the participating vehicles in the neighborhood share PVT-related data with the target vehicles employing low-cost receivers. The NMEA 0183 messaging protocol is an international data format intended for communication between electronic devices similar to the ASCII character standard for computer programming [1,14]. The NMEA messages are plain sentences with specific serial data fields that can be read by a common digital notepad and are composed of ASCII strings

that convey useful location-based information. A summary of the basic positioning metrics along with the corresponding NMEA messages is reported below [1,14]:

- Geographic latitude, longitude, and altitude ($GNGNS);
- Number of GNSS satellites in view ($GNGNS);
- Horizontal and vertical dilution of precision ($GNGNS);
- Horizontal and vertical accuracy standard deviations ($GNGST);
- Quality of the location (integrity, validity, and integer ambiguity status) ($GNGFA).

Especially, the $GNGST message is considered a significant requirement for high-precision GNSS positioning because of the role of GNSS metadata in evaluating the quality of GNSS coordinates. The low-cost GNSS receivers may transmit these NMEA messages through various short-range radio-communication interfaces such as the ITS technologies described in Table 1 as well as Wi-Fi, 3G, LTE-4G, 5G, and Bluetooth. The benefits of the NMEA protocol are numerous since it enables the communication between heterogeneous hardware and software while the users are not submitted to develop custom implementations for each GNSS receiver. In Figure 2, the operation of the proposed C-DGNSS framework is depicted.

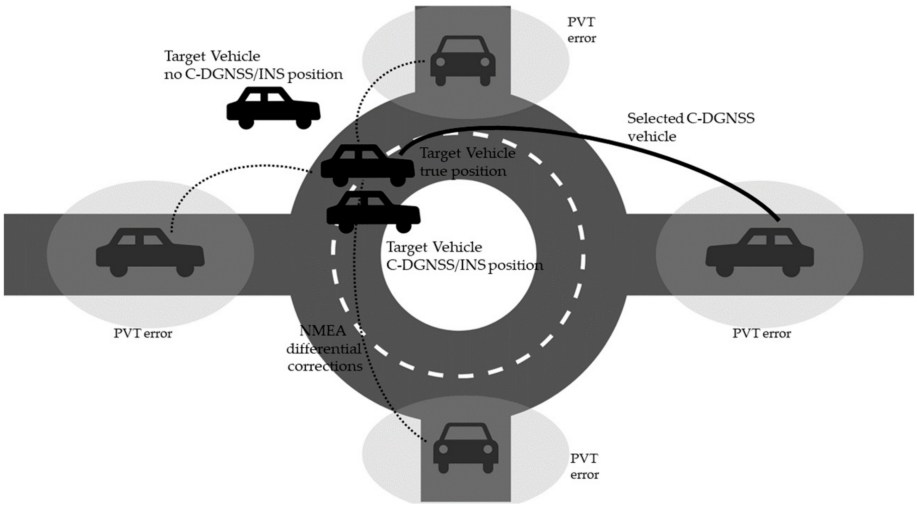

Figure 2. Diagram of the Cooperative-Differential GNSS (C-DGNSS) positioning configuration.

The aiding MADM module assists the target vehicle in selecting the best neighboring vehicle with which to cooperate and hence improves/updates its position in a realistic manner. It parses the incoming NMEA messages that constitute the criteria values of the decision matrix, and then the appropriate MADM algorithm takes over, providing rankings of the neighboring moving vehicles. The MADM module assumes a set of criteria or attributes that collectively define the GNSS position quality of the engaged cars. For the purpose of efficient C-DGNSS and achieving improved position accuracy with the lowest latency and cost, it is advisable that these attributes should be highly uncorrelated and up to 5 or 6.

From the reported NMEA messages described earlier, in our contribution, only certain fields are employed as input criteria for the proposed MADM module. Table 4 exhibits the list of criteria investigated per NMEA sentence: (1) The number of GNSS satellites in view (*NS*), (2) the root mean square of the double-difference phase residuals in the L1 band (*Range RMS*), (3) the standard deviation of the horizontal coordinates point fix (*Hz std*), (4) the standard deviation of the vertical coordinates point fix (*V std*), (5) the ambiguity status of the position solution (*Amb Stat*), and (6) the horizontal dilution of precision (*HDOP*). In greater detail, the *Range RMS* is measured in meters, the *Hz std* and *V std* are measured in meters and express the horizontal and vertical accuracy error in the position, and the *Amb Stat* denotes the GNSS receiver's integer ambiguity status. Thus, *Amb Stat* may yield an autonomous solution, a differential GNSS, a float solution, and

a high-resolution fixed solution. Finally, the *HDOP* reveals the effect of the DOP on the horizontal position value. The more satellites that are visible and low in the sky, the better the *HDOP* and the horizontal position (latitude and longitude). Finally, the criteria are of type "Expenses" or "Benefits". The first type implies that the lower the criterion value, the better (minimum), while the second type implies that the higher the criterion value, the better (maximum).

Table 4. Criteria used for implementing MADM technique in C-DGNSS positioning.

a/a	Criteria Name	NMEA Sentence	NMEA Field No	Type
1	Number of satellites (NS)	GNS	7	Benefit
2	Range RMS (L1 RMS)	GST	2	Benefit
3	Horizontal std (Hz std)	GST	6,7	Expense
4	Vertical std (V std)	GST	6,7	Expense
5	Integer ambiguity status (Amb Stat)	GNS	6	Benefit
6	Horizontal dilution of precision (HDOP)	GNS	8	Expense

The experimental NMEA PVT data used for the simulation and evaluation of our contribution were recorded from six land vehicles that drove concurrently over nonidentical trajectories that endured approximately 2000 epochs at a 1 Hz sampling rate (33.3 min in total) [27]. The collected trajectories' data are GNSS observations from various outdoor areas, including: (i) unobstructed, open space conditions, (ii) urban settings with narrow lanes and tall buildings, and (iii) semi-urban sections with grown trees and thick vegetation, causing a large-scale signal degradation and restricted view of the GNSS satellites [27]. Evidently, all vehicles carry a single low-cost GNSS receiver aboard able to compute the position solution and produce NMEA GNS and GST sentences. The first vehicle (veh. #1) is notated as the target vehicle, and the other five (veh. #2, veh. #3, veh. #4, veh. #5, and veh. #6) are considered the aiding vehicles. The MATLAB® toolbox was employed to import the data and establish a simulation environment for the MADM algorithms.

4.2. Comparative Analysis

In this section, thirteen MADM algorithms are simulated with various weightings, normalization techniques, and criteria associated with positioning accuracy employing experimental NMEA data time series. A comparative analysis is provided through an evaluation of the MADM algorithms in terms of ranking performance and robustness. An investigation of the importance and criticality of the criteria is also presented (sensitivity analysis), accompanied by the necessary ranking diagrams and simulation results.

The investigated methods are the SAW, CODAS, COPRAS, GRA, MABAC, D'IDEAL, TOPL1, TOPL2, TOPL3, VIKOR, ORESTE, PROMETHEE, and ELECTRE, where TOPL1 is the TOPSIS using the L1 norm or taxicab/Manhattan distance metric, TOPL2 employs the L2 norm, which is the Euclidean distance of each alternative from the best and worst ideal points, TOPL3 employs the infinite norm distance metric, while four distinct preference functions were employed for PROMETHEE.

The five alternative vehicles move in simultaneous but separate trajectories that span 2000 epochs. For each trajectory epoch, a decision matrix is formed with criteria values extracted from the NMEA sentences of the five aiding vehicles. Hence, a decision matrix associated with a specific timestamp (epoch) yields as many ranking results as the number of MADM algorithms and normalization techniques. In summary, in our MADM simulations, a trajectory of $T = 2000$ timestamps subject to $Q = 6$ criteria is examined employing $P = 5$ alternative vehicles (veh. #02–veh. #06) while the ranking results of 13 different MADM algorithms and five normalization techniques are reported. Table 5 exhibits the decision matrix with a of size (5×6) of a random timestamp filled with the required criteria values. The Amb Stat takes values of 1.0 for a fixed solution and 0.5 for a float solution.

Table 5. Decision matrix and criteria values of one timestamp.

a/a	NS	L1 RMS (m)	Hz std (m)	V std (m)	Amb Stat	HDOP
veh. #02	11	0.0030	0.0520	0.0320	0.5	0.66
veh. #03	10	0.0130	0.0160	0.0290	1.0	1.05
veh. #04	6	0.0040	2.9600	6.2380	0.5	1.77
veh. #05	8	0.0060	1.6930	2.2210	0.5	1.07
veh. #06	11	0.0040	0.0730	0.0420	0.5	0.66

Tables 6–9 present the simulations' ranking results after applying the MADM methods SAW, TOPL1, CODAS, and PROMETHEE, indicatively, with the criteria input data of Table 5. The index P_i represents the performance score of the i_{th} alternative, and A_i expresses the ID of the i_{th} alternative with i = 2, 3, 4, 5, and 6. It is observed that SAW, TOPL1, and CODAS produce identical rankings while PROMETHEE yields a slightly different top-three ranking. Moreover, the five normalization techniques are in good agreement with each other and with their corresponding ranking results.

Table 6. SAW.

Rank	**MAX**		**SUM**		**VEC**		**MAX-MIN**		**DEA**	
a/a	P_i	A_i	P_i	A_i	P_i	A_i	P_i	A_i	P_i	A_i
I	0.948	3	0.432	3	0.728	3	0.908	3	0.947	3
II	0.797	6	0.368	6	0.605	6	0.679	6	0.913	6
III	0.786	2	0.363	2	0.595	2	0.664	2	0.909	2
IV	0.589	5	0.257	5	0.441	5	0.401	5	0.731	5
V	0.289	4	0.094	4	0.194	4	0.016	4	0.499	4

Table 7. TOPL1.

Rank	**MAX**		**SUM**		**VEC**		**MAX-MIN**		**DEA**	
a/a	P_i	A_i	P_i	A_i	P_i	A_i	P_i	A_i	P_i	A_i
I	0.928	3	0.955	3	0.941	3	0.9081	3	0.8889	3
II	0.720	6	0.777	6	0.727	6	0.6798	6	0.7387	6
III	0.704	2	0.765	2	0.711	2	0.6645	2	0.7255	2
IV	0.433	5	0.468	5	0.444	5	0.4013	5	0.4094	5
V	0.017	4	0.015	4	0.018	4	0.0167	4	0.0145	4

Table 8. CODAS.

Rank	**MAX**		**SUM**		**VEC**		**MAX-MIN**		**DEA**	
a/a	P_i	A_i	P_i	A_i	P_i	A_i	P_i	A_i	P_i	A_i
I	0.948	3	0.432	3	0.728	3	0.908	3	0.947	3
II	0.797	6	0.368	6	0.605	6	0.679	6	0.913	6
III	0.786	2	0.363	2	0.595	2	0.664	2	0.909	2
IV	0.589	5	0.257	5	0.441	5	0.401	5	0.731	5
V	0.289	4	0.094	4	0.194	4	0.016	4	0.499	4

Table 9. PROMETHEE.

Rank	**V-SHAPE**		**LINEAR**		**GAUSSIAN**		**LIN-GAUS**	
a/a	P_i	A_i	P_i	A_i	P_i	A_i	P_i	A_i
I	1.378	2	1.166	2	0.953	2	1.009	2
II	1.366	6	1.166	6	0.951	6	1.008	6
III	1.016	3	1.000	3	0.816	3	0.920	3
IV	−1.106	5	−1.000	5	−0.657	5	−0.737	5
V	−2.655	4	−2.3333	4	−2.065	4	−2.201	4

Table 10 depicts the rank distribution (I-II-III-IV-V) among the alternative vehicles from all of the simulations incorporating all of the MADM methods and normalization techniques. Each column and each row add up to 100%. It is observed that veh. #03 is placed 85.7% in rank I; therefore, it is considered the optimal neighboring vehicle to receive the GNSS corrections for the specific epoch.

Table 10. All MADM simulations.

% Simulations	I	II	III	IV	V
veh. #02	14.3	3.2	82.5	0	0
veh. #03	85.7	1.6	12.7	0	0
veh. #04	0	0	0	0	100
veh. #05	0	0	0	100	0
veh. #06	0	95.2	4.8	0	0

The results derived from the total trajectory data using all of the MADM methods and normalization techniques are presented in Figure 3. The upper plot of Figure 3 assumes equal weights, whilst the bottom plot adopts a weight matrix $w = \begin{bmatrix} 0.1 & 0.2 & 0.2 & 0.2 & 0.2 & 0.1 \end{bmatrix}$. Obviously, the rankings of vehicles #02 and #04 remain almost the same, while the rankings of vehicles #03, #05, and #06 change slightly. Furthermore, vehicle #02 remains in rank I compared to other vehicles, and vehicle #04 remains in rank III along the trajectory.

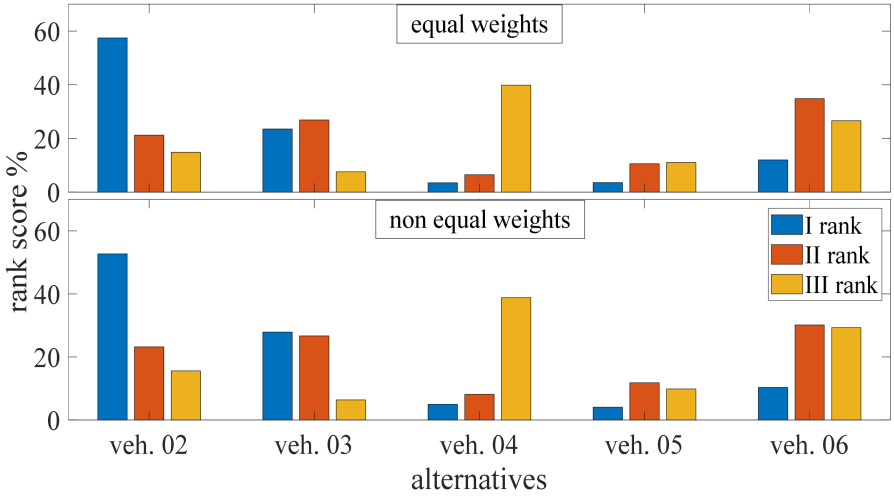

Figure 3. Mean ranking of I/II/III positions of alternative vehicles for the entire trajectory using all normalizations and 13 MADM methods. (**Top**) Equal weights; (**Bottom**) Unequal weights.

4.3. Sensitivity Analysis

In this sub-section, a sensitivity analysis is carried out to determine the most critical position-related criteria and to evaluate the robustness of the investigated MADM algorithms [24,25]. A sensitivity analysis can be performed for all the available methods, but in our case, only n = 3 MADM methods are compared: SAW, CODAS, and TOPL1, while m = 6 alternative vehicles are examined for a trajectory of k = 2000 epochs. Each epoch consists of data from i = 6 criteria, respectively: Number of satellites, L1 RMS double-difference phase residual, Hz std, V std, Amb Status, and HDOP indicator. Seven weight matrices are constructed: at first, a matrix with 1/6 equal weight for every criterion is formulated, and then six different weight matrices where each criterion weight is set to have a weight of 2/6 and the remaining criteria have equal weights. Thus, the weight matrices are presented analytically in Table 11.

Table 11. Weight matrices examined.

Case		Weight Vectors
Uniform Weighting	$w_0 =$	[1/6 1/6 1/6 1/6 1/6 1/6]
Importance on NS	$w_1 =$	[2/6 4/30 4/30 4/30 4/30 4/30]
Importance on L1 RMS	$w_2 =$	[4/30 2/6 4/30 4/30 4/30 4/30]
Importance on Hz std	$w_3 =$	[4/30 4/30 2/6 4/30 4/30 4/30]
Importance on V std	$w_4 =$	[4/30 4/30 4/30 2/6 4/30 4/30]
Importance on Amb Stat	$w_5 =$	[4/30 4/30 4/30 4/30 2/6 4/30]
Importance on HDOP	$w_6 =$	[4/30 4/30 4/30 4/30 4/30 2/6]

Every timestamp corresponds to a column that includes the ranking of alternative vehicles for each MADM method ($rank_{m/n}$), and thus the dimensions of the ranking matrix for every timestamp are (mxn). The subsequent step is the correlation coefficient matrix calculation using Spearman's correlation method between the ranking matrix obtained from the equal weight matrix w_0 with the results of the rest weight matrices (w_1, w_2, w_3, w_4, w_5, and w_6), where the result is a (nxi) matrix at every timestamp. In order to calculate the total correlation coefficient matrix from the complete trajectory, a sum along the third dimension is performed, and then it is divided by the total number of timestamps; this is the total correlation index (TCI). Conclusively, the criterion with the smaller TCI is the most sensitive one per each MADM method.

The Spearman's correlation coefficient *rho* between the two ranking vectors X, Y is given by:

$$rho(X,Y) = 1 - \frac{6\sum_{i=1}^{n} d_i^2}{n(n^2-1)} \tag{2}$$

where, d_i is the difference in the i_{th} rank between two ranking vectors (i.e., two MADM methods) and n is the length of each vector (number of alternatives). If the input is a ranking matrix X with multiple columns, $rho(\mathrm{X})$ returns a matrix with the correlations between each pair of its columns.

The Pearson's correlation coefficient ρ is a metric of the linear correlation between two random variables, X and Y, and it can be alternatively employed using the real-valued performance scores of the MADM methods instead of the integer-valued ranking vectors. It is defined as follows:

$$\rho(X,Y) = 1 - \frac{\sum_{i=1}^{n}\left(X_i - \overline{X}\right)\left(Y_i - \overline{Y}\right)}{\left\{\sum_{i=1}^{n}\left(X_i - \overline{X}\right)^2 \sum_{j=1}^{n}\left(Y_j - \overline{Y}\right)^2\right\}^{1/2}} \tag{3}$$

where $\overline{X}$, $\overline{Y}$ are the mean values and n is the length of each vector.

Table 12 summarizes Spearman's correlation results along the complete trajectory, where clearly, the smaller TCI values are observed in criteria L1 RMS double-difference phase residuals, HDOP, and Hz std, while the other criteria are less sensitive. Table 13 includes the Pearson's correlation results where the smaller TCI values are also spotted in criteria L1 RMS, HDOP, and V std, whereas the other criteria are slightly less sensitive. Concretely, Spearman's correlation coefficient is a more suitable tool to use for sensitivity analysis because the obtained TCIs differ a lot more, giving a definite ranking as compared to Pearson's TCIs, which mainly differ on the second and third decimal.

Table 12. Total Correlation Index (TCI) results using Spearman's correlation method.

Criterion	1	2	3	4	5	6
	Number of Satellites	**L1 RMS Double-Difference Phase Residuals**	**Hz std**	**V std**	**Amb Status**	**HDOP**
SAW	0.937	0.731	0.869	0.920	0.971	0.811
CODAS	0.894	0.613	0.761	0.821	0.944	0.723
TOPL1	0.937	0.731	0.869	0.920	0.971	0.811

Table 13. Total Correlation Index (TCI) results using Pearson's correlation method.

Criterion	1	2	3	4	5	6
	Number of Satellites	**L1 RMS Double-Difference Phase Residuals**	**Hz std**	**V std**	**Amb Status**	**HDOP**
SAW	0.996	0.969	0.995	0.994	0.995	0.988
CODAS	0.993	0.944	0.992	0.989	0.993	0.978
TOPL1	0.996	0.969	0.995	0.994	0.995	0.988

In Tables 14 and 15, the criteria from the most to least sensitive are sorted where the numbers 1–6 are the criteria IDs. L1 RMS (no. 2) is the most sensitive, followed by HDOP (no. 6).

Table 14. Criteria ranking from most to least sensitive using Spearman's correlation method.

Criteria Ranking	I	II	III	IV	V	VI
SAW	**2**	**6**	**3**	**4**	**1**	**5**
CODAS	2	6	3	4	1	5
TOPL1	2	6	3	4	1	5

Table 15. Criteria ranking from most to least sensitive using Pearson's correlation method.

Criteria Ranking	I	II	III	IV	V	VI
SAW	**2**	**6**	**4**	**3**	**5**	**1**
CODAS	2	6	4	3	1	5
TOPL1	2	6	4	3	5	1

5. Challenges and Future Research Trends

In this Section, the extension of the C-DGNSS concept beyond land-based vehicles is discussed, along with emerging challenges and future trends. Moreover, the "moving base station" technique can be fairly applied to drone positioning, drone-to-drone, drone-to-car communications, internet of drones (IoD), multi-UAV systems, UAV swarms, coordinated drones, and to improve their relative position accuracy further [28–30].

Considering a swarm of UAVs or a multi-UAV system, in order to maintain a coordinated and planned formation, a very accurate and efficient relative positioning method must be employed. Similar to land vehicles, open-sky conditions are favorable for GNSS-only positioning and navigation. On the other hand, in urban centers, the likelihood of an inner-system collision is high.

Future work will include low-cost C-DGNSS aided with a MADM module for drone vehicles in deep urban, suburban, and rural regions, simulations with experimental drone-to-car positioning measurements, and GNSS/INS integration in coordinated drone formations.

6. Conclusions

In this work, the challenge of efficient, accurate, and reliable CP, incorporating low-cost GNSS receivers in various critical ITS scenarios, was addressed. The C-DGNSS framework was employed, which is the classical D-GNSS coupled with CP between a target vehicle and a number of surrounding candidate neighbors. By retaining the properties of D-GNSS, the cooperating vehicles disseminate their PVT data and GNSS corrections from the available satellites in view through radio links. The main hypothesis is that the

target vehicle's low-cost receiver could improve both its relative and absolute positioning accuracy. The GNSS PVT information is comprised of NMEA messages, and the target vehicle parses the incoming NMEA sentences in a serial manner. With the aid of a MADM module, the target vehicle ranks and optimally decides in real-time which neighbors to select for retrieving GNSS corrections (RTCM data) to update its own PVT state. A set of thirteen MADM algorithms and several different normalization techniques were adopted for the simulation of scenarios involving various weightings and the criteria associated with positioning accuracy and ambiguities residual status. Real experimental criteria values derived from several low-cost GNSS receivers in complex driving environments were employed. A comparative analysis was then provided through an evaluation of the MADM algorithms in terms of ranking performance. A sensitivity analysis to determine the methods' robustness and the criticality of the criteria is also presented. It is concluded that L1 RMS, HDOP, and Hz std are the most critical, while the other criteria are less sensitive. Multi-purpose, generic applicability of the proposed scheme is suggested, not only for land vehicles, as it can be extended to drone positioning, swarm-of-entities guidance, drone-to-car communication, etc.

Author Contributions: Conceptualization, T.M., T.T.K., V.G. and A.D.P.; methodology, T.M. and T.T.K.; software, T.M.; validation, T.M. and T.T.K.; formal analysis, T.M. and T.T.K.; investigation, T.M. and T.T.K.; resources, T.M. and V.G.; writing—original draft preparation, T.M. and T.T.K.; writing—review and editing, A.D.P. and V.G.; visualization, T.M. and T.T.K.; supervision, A.D.P. and V.G.; funding acquisition, T.M. and V.G. All authors have read and agreed to the published version of the manuscript.

Funding: The research project was supported by the Hellenic Foundation for Research and Innovation (H.F.R.I.) under the "1st Call for H.F.R.I. Research Projects to support Faculty Members & Researchers and the procurement of high-cost research equipment grant" (Project Number: 2269).

Data Availability Statement: Not applicable.

Conflicts of Interest: The authors declare no conflict of interest.

References

1. Teunissen, P.; Montenbruck, O. (Eds.) *Handbook of Global Navigation Satellite Systems*; Springer International Publishing: Cham, Switzerland, 2017; pp. 1–1268. [CrossRef]
2. Gao, Z.; Ge, M.; Li, Y.; Shen, W.; Zhang, H.; Schuh, H. Railway Irregularity Measuring Using Rauch–Tung–Striebel Smoothed Multi-sensors Fusion System: Quad-GNSS PPP, IMU, Odometer, and Track Gauge. *GPS Solut.* **2018**, *22*, 22–36. [CrossRef]
3. Krasuski, K.; Savchuk, S. Determination of the Precise Coordinates of the GPS Reference Station in of a GBAS System in the Air Transport. *Commun. Sci. Lett. Univ. Zilina* **2020**, *22*, 11–18. [CrossRef]
4. Liu, W.; Shi, X.; Zhu, F.; Tao, X.; Wang, F. Quality Analysis of Multi-GNSS Raw Observations and a Velocity-aided Positioning Approach Based on Smartphones. *Adv. Space Res.* **2019**, *63*, 2358–2377. [CrossRef]
5. Specht, C.; Specht, M.; Dąbrowski, P. Comparative Analysis of Active Geodetic Networks in Poland. In Proceedings of the 17th International Multidisciplinary Scientific GeoConference (SGEM 2017), Albena, Bulgaria, 27 June–6 July 2017.
6. Specht, C.; Weintrit, A.; Specht, M. A History of Maritime Radio-navigation Positioning Systems Used in Poland. *J. Navig.* **2016**, *69*, 468–480. [CrossRef]
7. Alam, M.; Ferreira, J.; Fonseca, J.A. *Intelligent Transportation System (ITS), Dependable Vehicular Communications for Improved Road Safety*; Springer International Publishing: Cham, Switzerland, 2016; pp. 1–270. [CrossRef]
8. Meneguette, R.I.; De Grande, R.; Loureiro, A.A. *Intelligent Transport System in Smart Cities*; Springer International Publishing: Cham, Switzerland, 2018; pp. 1–182. [CrossRef]
9. *Report ITU-R M.2445-0*; Intelligent Transport Systems (ITS) Usage. International Telecommunications Union: Geneva, Switzerland, 2018.
10. Minetto, A.; Bello, M.C.; Dovis, F. DGNSS Cooperative Positioning in Mobile Smart Devices: A Proof of Concept. *IEEE Trans. Veh. Technol.* **2022**, *71*, 3480–3494. [CrossRef]
11. Antoniou, C.; Gikas, V.; Papathanasopoulou, V.; Mpimis, T.; Perakis, H.; Kyriazis, C. A Framework for Risk Reduction for Indoor Parking Facilities under Constraints using Positioning Technologies. *Int. J. Disaster Risk Reduct.* **2018**, *31*, 1166–1176. [CrossRef]
12. Chen, S.; Hu, J.; Shi, Y.; Zhao, L.; Li, W. A vision of C-V2X: Technologies, field testing, and challenges with chinese development. *IEEE Internet Things J.* **2020**, *7*, 3872–3881. [CrossRef]
13. Campolo, C.; Molinaro, A.; Scopigno, R. (Eds.) *Vehicular Ad Hoc Networks. Standards, Solutions, and Research*; Springer International Publishing: Cham, Switzerland, 2015; pp. 1–544. [CrossRef]

14. Koo, T.-Y.; Ji, S.-H.; Bae, C.-H.; Kim, H.-J.; Lee, J.-H.; Suh, M.-W. Development of the GPS Simulator for Driving Simulators. In Proceedings of the SICE-ICASE International Joint Conference, Busan, Korea, 18–21 October 2006; pp. 2133–2137. [CrossRef]
15. Karagiannis, G.; Altintas, O.; Ekici, E.; Heijenk, G.; Jarupan, B.; Lin, K.; Weil, T. Vehicular Networking: A Survey and Tutorial on Requirements, Architectures, Challenges, Standards and Solutions. *IEEE Commun. Surv. Tutor.* **2011**, *13*, 584–616. [CrossRef]
16. *Report ITU-R M.2228-1*; Advanced Intelligent Transport Systems (ITS) Radiocommunications. International Telecommunications Union: Geneva, Switzerland, 2015.
17. Arena, F.; Pau, G. An Overview of Vehicular Communications. *Future Internet* **2019**, *11*, 27. [CrossRef]
18. Xue, C.; Psimoulis, P.; Zhang, Q.; Meng, X. Analysis of the performance of closely spaced low-cost multi-GNSS receivers. *Appl. Geomat.* **2021**, *13*, 415–435. [CrossRef]
19. Elsheikh, M.; Abdelfatah, W.; Noureldin, A.; Iqbal, U.; Korenberg, M. Low-Cost Real-Time PPP/INS Integration for Automated Land Vehicles. *Sensors* **2019**, *19*, 4896. [CrossRef]
20. Ning, F.; Meng, X.; Wang, Y. Low-Cost Receiver and Network Real-Time Kinematic Positioning for use in Connected and Autonomous Vehicles. *J. Navig.* **2019**, *72*, 917–930. [CrossRef]
21. Chen, L.W.; Shih, H.W.; Tsai, M.F.; Deng, D.J. Finding Lane positions of vehicles: Infrastructure-less cooperative lane positioning based on vehicular sensor networks. *IEEE Veh. Technol. Mag.* **2015**, *10*, 70–80. [CrossRef]
22. Triantaphyllou, E. *Multi-Criteria Decision-Making Methods: A Comparative Study*; Springer Science+Business Media: Dordrecht, The Netherlands, 2000; pp. 1–290. [CrossRef]
23. Kraujalienė, L. Comparative analysis of multicriteria decision-making methods evaluating the efficiency of technology transfer. *Bus. Manag. Educ.* **2019**, *17*, 72–93. [CrossRef]
24. Kabassi, K. Application of Multi-Criteria Decision-Making Models for the Evaluation Cultural Websites: A Framework for Comparative Analysis. *Information* **2021**, *12*, 407. [CrossRef]
25. Pamučar, D.S.; Božanić, D.; Ranđelović, A. Multi-criteria decision making: An example of sensitivity analysis. *Serb. J. Manag.* **2017**, *12*, 1–27. [CrossRef]
26. Munjal, R.; Liu, W.; Li, X.; Gutierrez, J.; Chong, P.H.J. Multi-Attribute Decision Making for Energy-Efficient Public Transport Network Selection in Smart Cities. *Future Internet* **2022**, *14*, 42. [CrossRef]
27. Gikas, V.; Perakis, H. Rigorous Performance Evaluation of Smartphone GNSS/IMU Sensors for ITS Applications. *Sensors* **2016**, *16*, 1240. [CrossRef]
28. Abdelmaboud, A. The Internet of Drones: Requirements, Taxonomy, Recent Advances, and Challenges of Research Trends. *Sensors* **2021**, *21*, 5718. [CrossRef]
29. Shen, J.; Wang, S.; Zhai, Y.; Zhan, X. Cooperative relative navigation for multi-UAV systems by exploiting GNSS and peer-to-peer ranging measurements. *IET Radar Sonar Navig.* **2020**, *15*, 21–36. [CrossRef]
30. Wang, S.; Zhan, X.; Zhai, Y.; Chi, C.; Jia-Wen, S. Highly reliable relative navigation for multi-UAV formation flight in urban environments. *Chin. J. Aeronaut.* **2021**, *34*, 257–270. [CrossRef]